THE JOURNAL OF BIOLOGICAL CHEMISTRY VOL. 284, NO. 49, pp. 33957–33965, December 4, 2009

Translocation and Endocytosis for Cell-penetrating Peptide Internalization[S]

Received for publication, August 15, 2009, and in revised form, October 12, 2009 Published, JBC Papers in Press, October 15, 2009, DOI 10.1074/jbc.M109.056309

Chen-Yu Jiao[1], **Diane Delaroche, Fabienne Burlina, Isabel D. Alves, Gérard Chassaing, and Sandrine Sagan**[2]
From the Laboratoire des Biomolécules, Université Pierre et Marie Curie (Paris 6), 75005 Paris, France

Cell-penetrating peptides (CPPs) share the property of cellular internalization. The question of how these peptides reach the cytoplasm of cells is still widely debated. Herein, we have used a mass spectrometry-based method that enables quantification of internalized and membrane-bound peptides. Internalization of the most used CPP was studied at 37 °C (endocytosis and translocation) and 4 °C (translocation) in wild type and proteoglycan-deficient Chinese hamster ovary cells. Both translocation and endocytosis are internalization pathways used by CPP. The choice of one pathway versus the other depends on the peptide sequence (not the number of positive changes), the extracellular peptide concentration, and the membrane components. There is no relationship between the high affinity of these peptides for the cell membrane and their internalization efficacy. Translocation occurs at low extracellular peptide concentration, whereas endocytosis, a saturable and cooperative phenomenon, is activated at higher concentrations. Translocation operates in a narrow time window, which implies a specific lipid/peptide co-import in cells.

Cell-penetrating peptides (CPPs)[3] that share the activity of cellular entry are usually short peptides of less than 20 amino acids highly enriched in basic residues. Among them, Antp, Tat-(48–60), and oligoarginine peptides are the most intensively studied. Despite the wide use of these CPPs as macromolecular delivery devices, the internalization mechanism of these peptides in cells still remains largely controversial. The energy dependence of the internalization mechanism is unique because all endocytotic pathways are inhibited at low temperature. Consequently, at low temperature, internalization likely reflects a direct translocation mechanism. Early studies proposed that Antp enters cells by an energy-independent membrane translocation mechanism (1). This first analysis was then contradicted by other studies that suggested, with the use of inhibitors, the involvement of endocytosis in the cellular internalization of cell-penetrating peptides (2–4).

The hypothesis that endocytosis was the only internalization mechanism of CPP resulted from studies examining whether the temperature or the binding to cell-surface glycosaminoglycans (GAGs) were critical for peptide internalization. Most of these interpretations resulted from fluorescence microscopy data. For instance, it was reported that Antp, Tat, and oligoarginine peptides were not efficiently internalized in the Chinese hamster ovary (CHO) mutant pgsA-745 cell line, which does not produce cell-surface heparan sulfate or chondroitin sulfate (5, 6). However, recent data indicates that Tat-mediated transduction occurs in the absence of heparan sulfate and chondroitin sulfate (7). The discrepancies observed between studies may be explained in part by different incubation conditions (peptide/cells ratio and peptide concentration) (8), limits in fluorescence imaging, such as quenching (9), or fluorophore-dependent intracellular trafficking (10), as well as the possibility that endocytosis inhibitors might have nonspecific effects (11). Altogether, the existence of multiple internalization pathways was often suggested rather than demonstrated (12).

Using the mass spectrometry-based protocol we have reported to quantify the cellular uptake of peptides (13, 14), we have analyzed herein the internalization and the membrane-binding of CPPs to wild type CHO (K1) and GAG-deficient CHO (pgsA-745) cells. Internalization and membrane-binding have been studied at 37 °C (endocytosis and translocation) and 4 °C (translocation). Cell-penetrating peptides with a different number of positively charged amino acids (see Fig. 1) were studied: (+7), Antp; (+7), an Antp analogue P1; (+7), (RW)9; (+8), Tat; and (+9), Arg^9. To clarify the internalization mechanisms, kinetics of Antp analogue P1 internalization, the role of the extracellular peptide concentration, together with the impact of a specific phosphatidylinositol 4,5-diphosphate (PtdIns-4,5-P2) intracellular membrane binder on peptide internalization were also analyzed with the two cell types. Analysis of CPP intracellular distribution also has been visualized by confocal microscopy imaging.

Our results clearly demonstrate that cell-penetrating peptides use endocytosis and translocation to internalize into cells. The balance between the two pathways depends strongly on the peptide sequence (and not directly on the number of positive charges), on the extracellular peptide concentration, and on the negatively charged cell-surface components, GAGs. In addition, the high affinity of cell-penetrating peptides for cell-surface components is not related to their internalization efficiency. Surprisingly, not only endocytosis but also translocation occurred within a restricted time window, an observation that

[S] The on-line version of this article (available at http://www.jbc.org) contains supplemental Figs. 1 and 2.

[1] Recipient of a Ph.D. fellowship from the French Ministere de l'Enseignement Superieur et de la Recherche.

[2] To whom correspondence should be addressed: Université Pierre et Marie Curie-Paris 6, Unité Mixte de Recherches 7203 CNRS, École Normale Supérieure, 4 Place Jussieu, F-75005 Paris, France. Fax: 33-1-44-27-71-50; E-mail: sandrine.sagan@upmc.fr.

[3] The abbreviations used are: CPP, cell-penetrating peptide; CHO, Chinese hamster ovary; GAG, glycosaminoglycan; DMEM, Dulbecco's modified Eagle's medium; MALDI-TOF, matrix-assisted laser desorption ionization time-of-flight; MS, mass spectrometry; msr, mass stable reporter tag; PtdIns-4,5-P2, phosphatidylinositol 4,5-diphosphate; GM3, NeuAcα2,3Galβ1,4Glc ceramide.

gave evidence for a cell-penetrating peptide/lipid co-transport limiting step. Finally, GAG-mediated endocytosis is a cooperative and saturable process. Together, these results shed new light on the mechanisms of cell-penetrating peptide internalization and on the associated membrane components.

EXPERIMENTAL PROCEDURES

Reagents—Standard *t*-butoxycarbonyl amino acids, 4-methylbenzhydrylamine hydrochloride salt polystyrene resin, and 2-(1*H*-benzotriazole-1-yl)-1,1,3,3-tetramethyluronium hexafluorophosphate were purchased from Senn Chemicals. Solvents (peptide synthesis grade), *N*,*N*′-dicyclohexyhexylcarbodiimide, *N*-hydroxybenzotriazole, and (7-azabenzotriazol-1-yloxy)tripyrrolidinophosphonium hexafluorophosphate were obtained from Applied Biosystems. 1-Hydroxy-7-azabenzotriazole was purchased from Fluka. 98% *N*-*t*-butoxycarbonyl[2,2-^{2}H]glycine was obtained from Cambridge Isotope Laboratories. 4-Benzoylbenzoic acid was obtained from Acros Chemistry.

Solid-phase Peptide Synthesis—Peptides were assembled by stepwise solid-phase synthesis on an ABI 433A peptide synthesizer (Applied Biosystems) using a standard *t*-butoxycarbonyl strategy (4-methylbenzhydrylamine hydrochloride salt polystyrene resin, with a loading of 0.9 mmol NH_2/g, amino acid activation with *N*,*N*′-dicyclohexyhexylcarbodiimide/*N*-hydroxybenzotriazole or 2-(1*H*-benzotriazole-1-yl)-1,1,3,3-tetramethyluronium hexafluorophosphate) on a 0.1-mmol scale (11, 16). The *m*/*z* of the protonated molecule (first isotope) are given as experimental (theoretical): ^{1}H-Antp, 2699.3 (2699.5); ^{2}H-Antp, 2707.3 (2707.5); ^{1}H-P1, 3068.6 (3068.3); ^{2}H-P1, 3076.6 (3076.4); ^{1}H-msr(R/W)9, 2339.7 (2339.2); ^{2}H-msr(R/W)9, 2349.7 (2349.3); ^{1}H-(Arg)9, 1877.2 (1877.1); ^{2}H-(Arg)9, 1885.2 (1885.1); ^{1}H-Tat, 2115.2 (2115.1); and ^{2}H-Tat (2123.2).

Cell Culture—Wild type (CHO-K1) and xylose transferase-deficient (pgsA745) Chinese hamster ovary cells were obtained from the American Type Culture Collection (Manassas, VA). All cell lines were grown under an atmosphere of 5% CO_2 in air and 100% relative humidity in F12 growth medium (DMEM) supplemented with 10% (v/v) fetal bovine serum, 100 μg/ml of streptomycin sulfate, amphotericin B, and 100 units/ml of penicillin G.

Measure of the Cellular Uptake by MALDI-TOF MS—The internalization experiments were performed as described previously (13, 14). All cell-penetrating peptides contained an isotope tag on the N terminus (Biotin-GGGG or msr; see Figs. 1 and 2) to allow absolute quantification by MALDI-TOF MS. CPPs were synthesized with the nondeuterated (^{1}H-peptide) and deuterated tag (^{2}H-peptide).

One million adherent cells were incubated with the cell-penetrating ^{1}H-peptide in culture medium (without fetal calf serum) at 4 or 37 °C (see Fig. 2). After washing with culture medium, trypsin or pronase was added to degrade the remaining extracellular and membrane-bound peptide and to detach cells. After addition of enzyme inhibitors mixed with bovine serum albumin cells were transferred to a microtube, centrifuged, and washed with Tris buffer. The cells were then lysed in a solution containing a controlled and relevant quantity of the chemically identical deuterated form (^{2}H) of the CPP (which served as internal standard to quantify the internalized amount of ^{1}H-CPP). The sample was then boiled for 15 min to kill protease activity and to destroy potential CPP intracellular partners molecular interactions. The CPPs (^{1}H and ^{2}H) were then purified with streptavidin-coated magnetic beads eluted in the α-cyano-4-hydroxy cinnamic acid matrix before MALDI-TOF MS analysis. The amount of intact internalized peptide was calculated from the area ratio of the $[M + H^+]$ signals of intact ^{1}H-peptide and ^{2}H-peptide. The ^{1}H- and ^{2}H-peptides were separated by 8 atomic mass units, so there was no overlap of their signals on the mass spectra. As for standard quantity, we found quantification to be more accurate when the ^{1}H-CPP/^{2}H-CPP signals ratio ranged from 0.2 to 5. In addition, for each experiment, we used duplicate or triplicate wells, and the experiments were repeated independently at least three times, as indicated in the figures. Amounts of intact peptide from ~0.5 pmol could be measured without upper limit. This corresponds to intracellular concentrations of ~0.5 μM (mean volume of one CHO cell, 1 picoliter).

For neomycin assays, cells were preincubated for 30 min with 10 mM of neomycin, prior to peptide incubation. For all assays, after peptide incubation, cells were washed three times with 1 ml DMEM, treated with trypsin (37 °C) as described previously, or with 0.05% pronase (37 or 4 °C) in 100 mM Tris, pH 7.5. The samples were analyzed by MALDI-TOF MS (positive ion reflector mode) on a Voyager DEPRO mass spectrometer (Applied Biosystems).

Confocal Microscopy—7.5×10^4 cells were cultured on coverglass in 24-well plates in DMEM. After washing with culture medium DMEM, cells were incubated for 1 h in 1 ml of 5 μM of the biotinylated peptide at the indicated temperature. Cells were then labeled as described (16). CLSM was performed on an inverted LSM510 laser-scanning microscope (Carl Zeiss).

Sialic Acid Quantification—A sialic acid quantification kit was purchased from Sigma-Aldrich. CHO cells were harvested from confluent 225 cm^2 tissue culture flasks. Sialic acid was measured spectrophotometrically at 340 nm according to the manufacturer's protocol.

RESULTS

Pronase Instead of Trypsin Could Be Used to Digest Membrane-bound Peptides at 4 °C—Internalization was studied at the kinetic plateau previously determined to be ~30 – 45 min (15). Therefore, the peptides Antp, P1, (R/W)9, R9, and Tat (Fig. 1) were incubated for 60 min, with cells at 37 °C before quantification by MALDI-TOF MS (Fig. 2). As the protocol of quantification was first settled down with trypsin, we had to assay another enzyme that could digest peptides at 4 °C. Therefore, the quantification protocol has been first assayed at 37 °C with trypsin or pronase in parallel. Similar intracellular peptide quantities were measured with trypsin (Fig. 3*A*) or pronase (Fig. 3*B*) in the two cell lines, with the exception of R9. Indeed, after pronase digestion, the amount of cell-associated R9 was twice the value obtained after trypsin digestion. However, this 2-fold increase was observed in the two cell lines. Therefore, pronase was used for further quantification performed in parallel at 4 and 37 °C in wild type and xylose transferase-deficient cells.

Antp: Biot-G_4-RQIKIWFQNRRMKWKK-NH_2

P1: Biot-G_4- (Nε-bzp)KRQIKIWFQNRRMKWKK-NH2

R9: Biot-G_4-R_9-NH_2

Tat: Biot-G_4-RKKRRQRRRPPQ-NH_2

(R/W)9: CF_3-NH-C(CH_2CH_3)$_2$-(NεBiot)K-(D)KCRRWWRRWRR-NH_2

msr

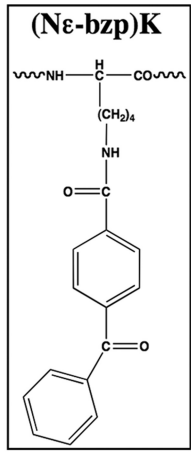

FIGURE 1. **Cell-penetrating peptide sequences used in this study.** *Biot*, biotin.

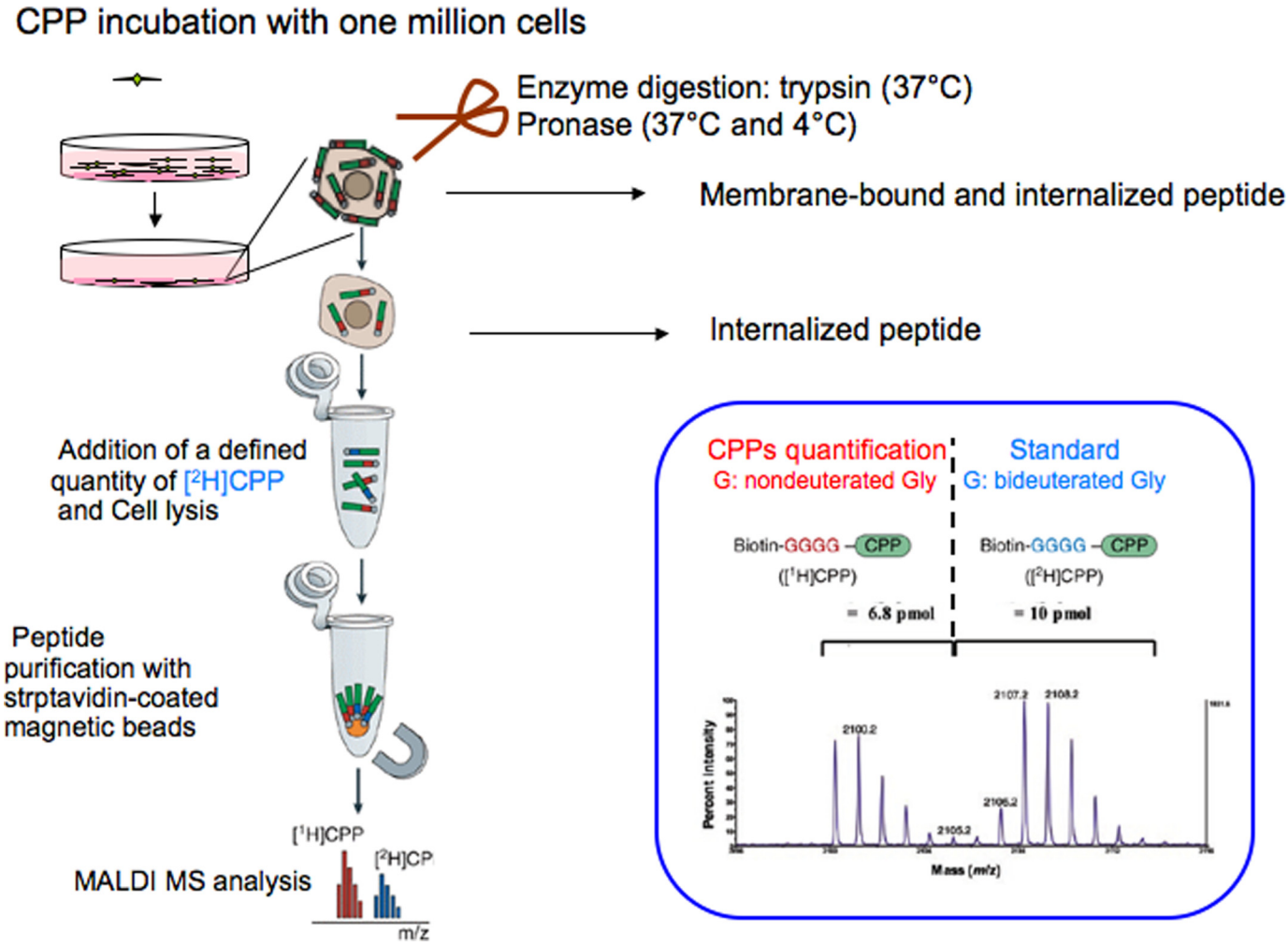

FIGURE 2. **Protocol of peptide quantification.** The protocol used in this study is described under "Experimental Procedures." Further detail can be found in Refs. 13 and 14.

Cell-penetrating Peptides Are Internalized at 4 °C in Wild Type and Mutant Cells—In CHO-K1 cells, internalization of the different cell-penetrating peptides was differently affected by the temperature decrease (Fig. 3*B*). Indeed, when temperature was decreased to 4 °C, the internalization of 5 μM Antp or its analogue P1 was significantly inhibited by 68%, whereas for R9 and (R/W)9, internalization was reduced by 49 and 90%, respectively. In contrast, the decrease in Tat entry was not found significant.

The situation was different with mutant GAG-deficient cells, in which the internalization of R9, Tat, and P1 was slightly affected by decreasing the temperature from 37 to 4 °C, whereas

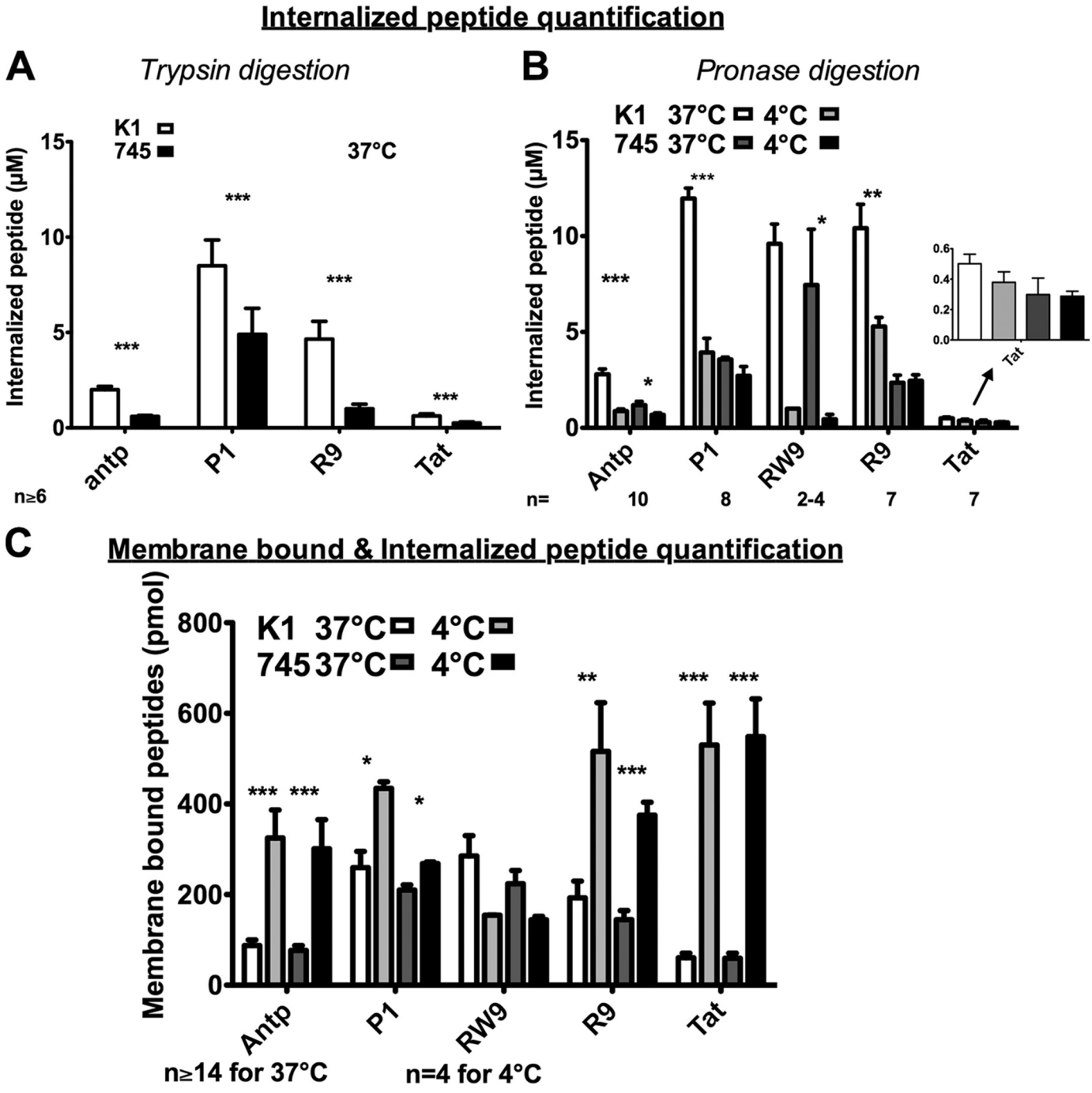

FIGURE 3. **Quantification of internalized and membrane-bound cell penetrating peptides in CHO-K1 and CHO-pgsA-745 cells.** *A*, internalized concentrations in wild type (K1) and xylosyltransferase I-deficient (745) CHO cells. One million cells were incubated with peptides for 75 min at 37 °C. The membrane-bound peptide was digested with trypsin. *B*, temperature effect on the amount of internalized peptide. One million cells were incubated with peptides during 75 min at 37 or 4 °C. The membrane-bound peptide was digested with pronase. *C*, temperature effect on the membrane-bound and internalized peptides. One million cells were incubated with peptides during 75 min at 37 or 4 °C. Cells were washed three times with culture medium. Extracellular concentration of peptides in *A*, *B*, and *C*: 2 μM for (R/W)9; 5 μM for Antp, P1, and R9; and 7.5 μM for Tat. *Columns from left to right*, K1, 37 °C; K1, 4 °C; 745, 37 °C; and 745, 4 °C. *Error bars* are S.E. obtained from *n* independent experiments. Differences in peptide quantity measured at 37 and 4 °C were: ∗, significant ($0.01 < p < 0.05$); ∗∗, very significant ($0.001 < p < 0.01$); and ∗∗∗, highly significant ($p > 0.001$).

Antp and (R/W)9 internalization was inhibited by 42 and 90%, respectively. Altogether, with the exception of (R/W)9 and R9, the quantity of peptide internalized at 4 °C in wild type cells was found very similar to the quantity internalized in mutant cells at 37 and 4 °C.

Decreasing the Temperature from 37 to 4 °C Leads to an Increased Quantity of Membrane-bound Peptides to the Two Cell Types—Peptides were also incubated for 60 min with cells, but trypsin or pronase digestion was omitted. In this experiment, the amounts measured thus corresponded to the sum of the internalized peptide as well as the peptide bound to the membrane, which could not be eliminated with DMEM washing (Fig. 3*C*). With the exception of (R/W)9, decreasing the temperature from 37 to 4 °C led to an increase

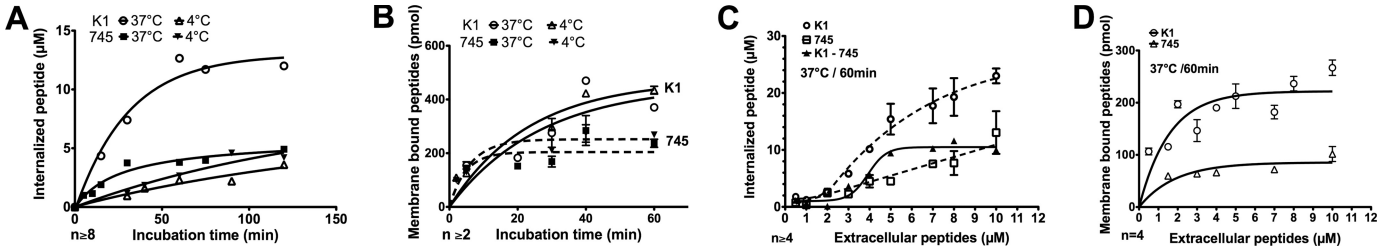

FIGURE 4. **Kinetics and concentration dependence.** Kinetics of peptide internalization (*A*) and binding to membrane (*B*). CHO-K1 or CHO-pgsA-745 cells were incubated, at 37 or 4 °C, with 5 μM extracellular peptide (P1) for the indicated incubation times. Effect of extracellular peptide concentration on internalized (*C*) or membrane-bound (*D*) peptide quantity. CHO-K1 or CHO-pgsA-745 cells were incubated with different concentrations of peptide (P1) during 60 min at 37 or 4 °C. *Error bars* are S.E. obtained from *n* independent experiments.

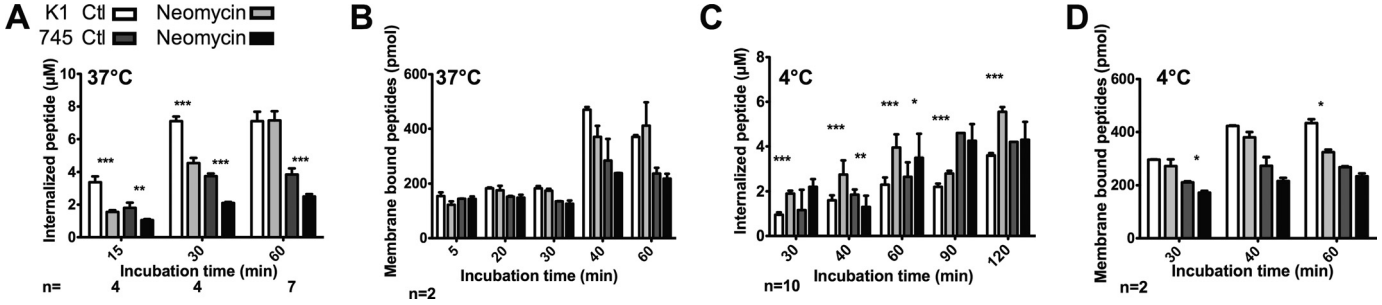

FIGURE 5. **Effect of neomycin on peptide internalization (*A* and *C*) or binding to membrane (*B* and *D*).** CHO-K1 or CHO-pgsA-745 cells were pretreated with 10 mM neomycin for 30 min, washed, and additionally incubated at 37 °C (*A* and *B*) or 4 °C (*C* and *D*) with 5 μM extracellular peptide (P1) for the indicated incubation times. *Error bars* are S.E. obtained from *n* independent experiments.

in membrane-bound peptides, to the same extent in wild type and xylose transferase-deficient cells: 4-fold for Antp, 1.5-fold for P1, 2.5-fold for R9, and 9-fold for Tat. In contrast, the affinity of (R/W)9 was not significantly different for the two membrane cell lines.

Kinetics of Internalization and Binding to Cell Membrane Are Affected by Temperature—We further analyzed the effects of temperature on internalization in the two cell lines (Fig. 4). The kinetics of internalization were analyzed with the Antp analogue P1, which behaved similarly to Antp in terms of temperature-dependent internalization in the two cell lines. This Antp analogue has the great advantage of having higher internalization quantity than the original peptide. Therefore, discrete differences in internalization kinetics would be better perceived with this peptide. As shown in Fig. 3*A*, the internalization rate and efficacy in wild type cells were temperature-dependent. Indeed, at 37 °C, the internalization kinetics reached the steady state after 50 min with a final intracellular concentration of ~12 μM. At 4 °C, the uptake kinetics was slowed down and reached a plateau after 60 min. However, the internalized peptide concentration at the plateau was 3-fold less than that measured at 37 °C, which was 4 μM.

A different situation occurred with mutant cells. At 37 °C, the plateau was attained after 30 min with an internalized maximal concentration of 4 μM. At 4 °C, the rate of internalization was similar to the one observed in wild type cells. The kinetics of entry reached the steady state after 60 min, which corresponded to 4 μM of internalized peptide.

Kinetic analysis of the membrane-associated Antp analogue P1 is shown in Fig. 4*B*. For incubation times over 20 min, the amount of membrane-bound peptide was always superior with CHO-K1 cells than with mutant cells. Additionally, a slightly higher affinity of P1 for the cell membrane was observed at 4 °C when compared with 37 °C, in both cell types.

Concentration Dependence of the Internalization Leads to Discriminate Translocation from Endocytosis—To further dissect the mechanisms involved in the internalization of the Antp analogue P1 in wild type and mutant cells, we have followed the internalized peptide as a function of the extracellular peptide concentration (Fig. 4). We have used (Fig. 4*C*) peptide concentrations ranging from 0.5 to 10 μM. In wild type cells, internalization according to extracellular peptide concentrations could be fitted to a cooperative sigmoidal-like curve that did not saturate (Fig. 4*C*). In contrast, in mutant cells, internalization according to the extracellular concentration best fitted a linear regression line ($y = 1.2x$, $r = 0.91$). At concentrations below 2 μM and higher than 5 μM, the two curves were parallel lines, merging below 2 μM and being equidistant above 5 μM. This observation demonstrated that the role of heparan and chondroitin sulfate in internalization was limited and saturating. When the two curves were subtracted, a pure cooperative and saturating sigmoidal curve could indeed be observed (Fig. 4*C*). Therefore, at concentrations below 2 μM, the internalization efficiency was the same in wild type and mutant cells.

Similarly, the amount of membrane-bound peptide was measured as a function of extracellular peptide concentrations in the two cell lines (Fig. 4*D*). The quantity of membrane-bound peptide was found to be concentration-dependent and reached a maximum at 5 μM extracellular peptide concentration in wild type cells. In contrast, in mutant cells, saturation of the membrane binding sites was attained with 2 μM extracellular peptide concentration. At concentrations

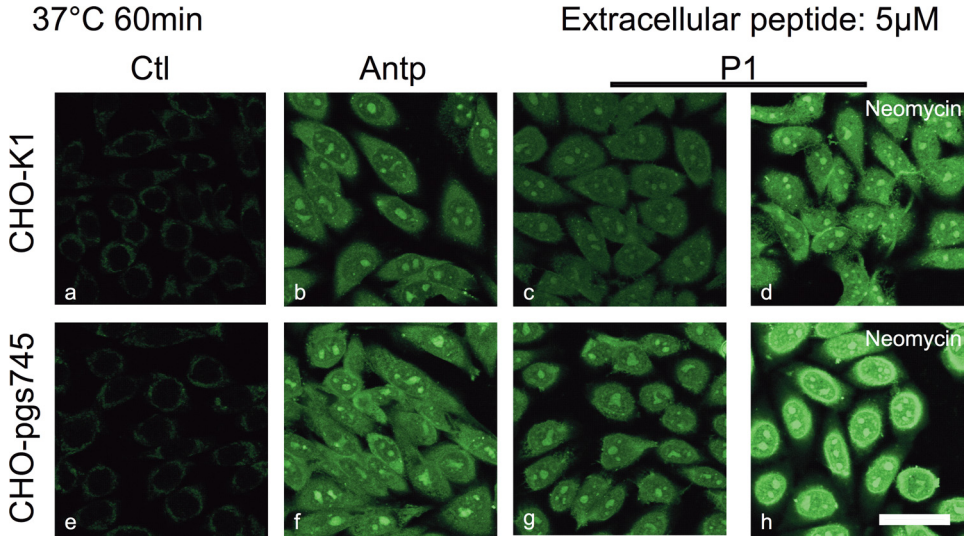

FIGURE 6. **Confocal microscopy of Antp and P1 internalization at 37 °C.** CHO-K1, CHO-pgsA-745, plated on glass coverslips, were incubated for 60 min with Antp (*b* and *f*) or P1 (*c*, *d*, *g*, and *h*) (5 μM). For *d* and *e*, cells were preincubated with 10 mM neomycin for 30 min. Cells were fixed with paraformaldehyde; biotinylated peptides were labeled with streptavidin-Alexa Fluor 488. *Scale bar*, 50 μM. *a*, control cells without peptide incubation.

above 5 μM, the membrane binding sites in mutant cells represented ~37% of those measured in wild type cells.

Specific Intracellular PtdIns-4,5-P2 Membrane Binder, Neomycin, Affects Internalization—Neomycin was preincubated with cells at 37 °C for 30 min prior to internalization assays at 37 (Fig. 5*A*) or 4 °C (Fig. 5*C*) with the Antp analogue P1 or (R/W)9. The antibiotic had different effects on peptide internalization in the two cell types according to temperature.

The rate of internalization was slowed down by 53% (15 min) in wild type cells and 37% (30 min) in neomycin-treated cells (both at at 37 °C), but this effect was surmountable after a 1-h incubation (Fig. 5*A*). In mutant cells, the effect was different because pretreated cells had a constant and lower (~35%) internalization efficiency compared with control cells, within the 1-h incubation with the peptide.

The situation was different at 4 °C (Fig. 5*A*). In wild type cells pretreated with neomycin, the P1 analogue had significantly enhanced internalization efficiency (~150%) compared with control cells, whatever the time incubation with the peptide. On the contrary, internalization efficiency of P1 at 4 °C in the mutant cells was not affected by the presence of neomycin.

Neomycin also Slightly Affects the Quantity of Membrane-bound Peptide—The effect of neomycin on the amount of membrane-bound peptide has also been examined in the two cell lines according to temperature (Fig. 5, *B* and *D*).

At 37 °C (Fig. 5*B*), the pretreatment of cells with neomycin did not show any effect on the membrane-bound peptide as similar quantities were found whatever the internalization time for the two cell lines. On the contrary at 4 °C (Fig. 5*D*), a slight (25%, corresponding to 100 pmol) but significant decrease on the membrane-bound peptide could be observed for the wild type cells after a 1-h internalization. A slight decrease was also observed constantly in mutant cells but corresponded only to 40 picomoles of membrane-bound peptide.

Confocal Microscopy Imaging Does Not Reflect the Internalized Peptide Quantity—Cells were incubated with 5 μM Antp or P1 analogue at 37 °C for 1 h with wild type or mutant cells (Fig. 6). Internalization of the peptide was revealed by streptavidin-Alexa Fluor 488 after quenching of the membrane-bound peptide by avidin as described (16). The confocal microscopy observations were all performed with the same microscopy tuning parameters. Antp and its P1 analogue were visualized both in wild type (Fig. 6, *b* and *c*, respectively) and mutant cells (Fig. 6, *f* and *g*, respectively). To compare with the data obtained from quantitative analysis of internalization, the two cell lines were also pretreated for 30 min with neomycin before P1 peptide analogue incubation (Fig. 6, *d* and *h*). When using the same observation parameters, fluorescence appeared more intense in cells pretreated with neomycin (*d* and *h*) when compared with controls (*c* and *g*), whatever the cell line.

Under the same conditions, Antp was also internalized at 4 °C in the two cell lines (supplemental Fig. S1). At 5 or 10 μM Antp, the two cells lines had similar fluorescence levels.

The Sialic Acid Content in the Two Cell Lines Are Similar—The content in sialic acid was found similar (using the nonparametric Mann-Whitney test) in 10^7 wild type (10.9 ± 4.5 nmol, $n = 3$) and mutant CHO cells (6.0 ± 2.5 nmol, $n = 4$).

DISCUSSION

Cell-penetrating peptides could be quantified using mass spectrometry, either once internalized or when bound to the external leaflet of the membrane (13, 15). As described previously, one million cells were incubated with, for example, 7500 pmol of peptide in 1 ml total volume (corresponding to an extracellular concentration of 7.5 μM). This large volume was used to cover cells properly with a solution that could not be depleted in the peptide. Therefore, when a peptide is internalized in a quantity of ~0.5 picomole, the cell volume of one million CHO cells being 1 μl, the internalized concentration corresponds to 0.5 μM, a limit concentration that can be visualized by fluorescence microscopy (17). However, it must be noted that this low concentration represents ~300,000 peptide molecules inside one cell. Therefore, when five pmol Antp are internalized in one million cells, the intracellular and extracellular concentrations are almost balanced, 5 *versus* 7.5 μM, respectively. In addition, using Antp to convey a protein kinase C inhibitor inside cells, micromolar concentration of the cargo was obtained (18), which was sufficient to observe a biological activity (19). In addition, this quantitative method has the great advantage over imaging techniques of giving access to the molecular integrity of the CPP (15). In this study, no intracellular degradation of CPPs was detected (similar mass spectra

showing no degradation after internalization at 37 and 4 °C) within the time range of internalization (15–120 min) (data not shown) (14, 15, 17).

We have studied the internalization of cell-penetrating peptides bearing different numbers of positive charges (from 7–9) in two cell types. CHO-K1 cells have been reported to contain heparan and chondroitin sulfate proteoglycans, together with sialic acid present on *N*-glycosylated proteins and GM3, the only ganglioside found in CHO cells (20, 21), whereas in xylose transferase-deficient pgA745 CHO cells, the heparan and chondroitin sulfate proteoglycans are lacking (22). We have shown herein that the cell-surface sialic acid content was similar for the wild type and the xylose transferase-deficient cells, that is, ~1000 picomoles for one million cells, which is the number of cells used in quantification studies. Thus, differences between internalization in the two cell types could be reasonably related to the difference in cell-surface heparan and chondroitin sulfates.

CPP Internalization as a Multimechanism Process—The data obtained herein clearly established that internalization of cell-penetrating peptides is a multimechanism process, which varies with the peptide sequence and the cell-surface composition. Indeed, we have measured the internalization of cell-penetrating peptides with a different number of positive charges and amphipathicity: (+7), (R/W)9; (+7), Antp; (+7), P1; (+8), Tat; and (+9), R9 (see Fig. 1 for peptide primary sequences).

In CHO-K1 wild type cells, at least two pathways of entry coexist: a temperature-sensitive endocytotic and a temperature-insensitive or less sensitive (likely translocation) pathway. These two pathways are not equivalently taken by the CPPs studied here (Table 1 and Fig. 7). By assuming that all active endocytotic processes are inhibited at 4 °C, we could evaluate for equivalent concentrations of the different cell-penetrating peptides, the relative percentage of peptide translocation *versus* endocytosis (Table 1). It is clear from these results that the presence at the cell surface of heparan and chondroitin sulfate has different effects on internalization depending on the CPP sequence. Indeed, in the absence of heparan and chondroitin sulfate (GAG), Tat (+8) and R9 (+9) only entered via a nonendocytotic temperature-independent process, whereas in the presence of GAG, translocation represented 75 and 50% of the internalization pathway, respectively, for the two peptides. In the absence of GAG, Antp (+7) and P1 (+7) entered principally (60 and 75%, respectively) via translocation, whereas (R/W)9 (+7) still entered preferentially via endocytosis (85%). For Tat, these results are in agreement with recent work in which a knockdown of clathrin-mediated endocytosis and a knock-out of caveolin-mediated endocytosis did not affect the ability of Tat to enter cells, even at low temperature (23).

Relationship between High Affinity Membrane-binding Sites and Internalization Efficiency—In the absence of pronase digestion, which preserves the high affinity membrane binding sites (membrane-bound peptide resistant to washing), the quantity of cell-associated peptide varies with temperature and peptide sequence. As membrane trafficking occurs at 37 °C, it is not possible to draw conclusions on the relation between the CPP number of charges and its membrane affinity. However, at 4 °C (at which membrane trafficking is inhibited), the membrane binding according to the peptide sequence was enhanced from 1.5–9-fold, compared with the values obtained at 37 °C. The quantity of membrane-associated peptides can be ranked roughly according to the number of positive charges of the CPP: R9, (+9); Tat (+8) > Antp (+7); and P1 (+7) > (R/W)9 (+7) in both cell types. Thus, the high affinity membrane binding sites (resisting washing) of the cell-penetrating peptides involve principally electrostatic interactions, which, however, are not sufficient to explain further CPP internalization. Indeed, the intracellular peptide concentrations measured in parallel did not follow the same rank order.

TABLE 1

Translocation *versus* endocytosis given for one extracellular peptide concentration

The internalized quantity at 4 °C (translocation) over internalized quantity at 37 °C (translocation and endocytosis) gave the % of translocation for each peptide.

Extracellular [CPP] (number of + charges)	Wild type CHO-K1 cells		Heparan sulfate and chondroitin sulfate-deficient CHO cells	
	Translocation	Endocytosis	Translocation	Endocytosis
	%		%	
2 μM (R/W)9 (+7)	15	85	15	85
5 μM Antp (+7)	30	70	60	40
5 μM P1 (+7)	20	80	75	25
7.5 μM Tat (+8)	75	25	100	0
5 μM R9 (+9)	50	50	100	0

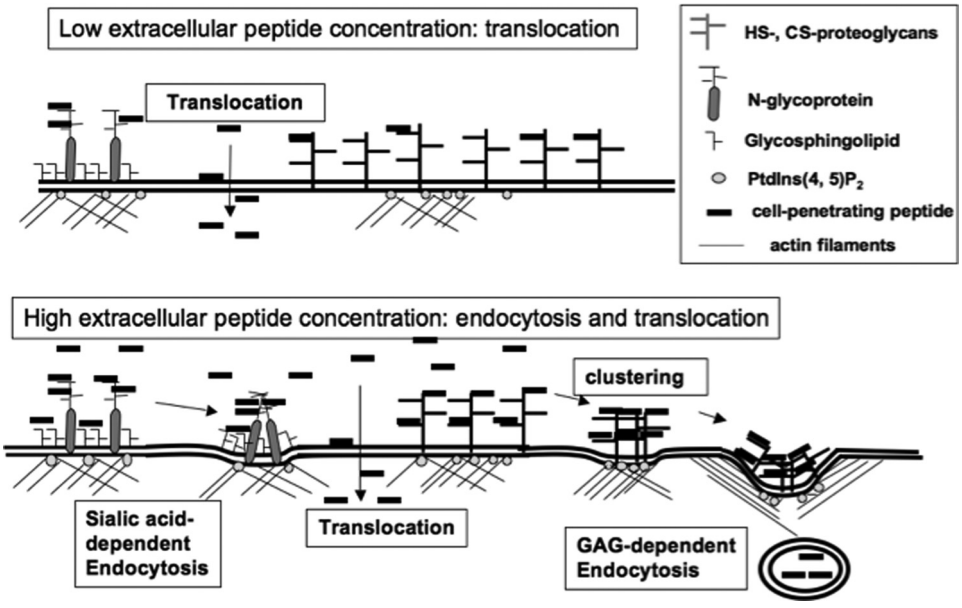

FIGURE 7. **Schematic representation of the different pathways of Antp internalization in cells.** At submicromolar concentrations, Antp translocates into cells. Translocation is accomplished by a co-transport mechanism, likely a negatively charged membrane lipid. At higher concentrations, in addition to translocation, the peptide accumulates on the cell surface, leading to GAG clustering and endocytosis.

Because the amount of the membrane-bound peptides was similar in the two cell-types these electrostatic interactions involved principally sialic acid (present on GM3 and *N*-glycoproteins) (20, 21). However, our results show that interactions with GAG are important for CPP endocytosis and that sialic acid binding sites are not necessarily competent for internalization. Indeed, with the exception of (R/W)9, endocytosis was almost fully inhibited in the absence of GAG (similar quantities internalized at 37 and 4 °C), an extreme case exemplifying this is Tat. Among all of the CPPs studied here, Tat showed the highest affinity for the cell membrane (at 4 °C), an affinity similar in both cell types, but was the least efficiently internalized CPP.

Antp Translocation Occurs at Low Micromolar Concentrations—The internalization mechanism was further dissected using the Antp analogue P1, which had the advantage over the other peptides of entering cells more efficiently. Therefore, it was easier to study the concentration dependence of internalization in the two cell types with this peptide. In contrast to recent reports (2–4, 24, 25), it is evidenced here that translocation occurs at lower concentrations as just reported for oligoarginine peptide (26) and thus should be a common feature of CPP. Endocytosis was observed at concentrations above 2 μM and could be described as a cooperative and saturable phenomenon that required accumulation of the peptide at the cell-surface proteoglycans and their clustering before endocytosis (Fig. 7) (27). Accordingly, the extended amount of time (several hours) required for turnover of heparan sulfate proteoglycan explains that we could observe this saturable endocytotic process, which also reached a steady state in kinetic study (28, 29). The fact that translocation also occurred in a narrow time window, as observed in kinetic studies, is of great importance. Indeed, this time-limited phenomenon implies that the cell-penetrating peptide had to recruit and use up specific membrane components, likely phospholipids or glycosphingolipids, to translocate with them into cells. These results support previous works on model membrane or in cells that already suggested that a limited and specific lipid/peptide import in cells (14, 30, 31).

In addition, internalization of Antp, P1, R9, and Tat did not involve fluid phase endocytosis (not saturable with respect to extracellular concentrations, linear with time, and inhibited at low temperature) evoked in raft domains (32). Indeed in GAG-deficient cells, the internalization of these CPPs was only slightly or not dependent on temperature and, in addition for the Antp analogue, was not linear with time. However, for (R/W)9, the possibility of the involvement of the fluid phase endocytosis cannot be ruled as the internalization of the peptide was slightly affected by the absence of GAG but was inhibited at low temperature in the two cell lines.

Importance of PtdIns-4,5-P2 in the Internalization Process—It is well documented that endocytosis occurs through proteoglycans or gangliosides, alone or associated with membrane *N*-glycoproteins (33). Actin stress fibers are involved in these endocytotic processes and are anchored to the internal leaflet of the membrane in lipid domains enriched in PtdIns-4,5-P2 (34–37). In addition, actin cytoskeleton dynamics are implicated in internalization of cell-penetrating peptides (38, 39). Thus, it was expected that neomycin, a positively charged aminoglycoside antibiotic, known to enter cells and to bind specifically to intracellular PtdIns-4,5-P2 (40, 41) could affect internalization of cell-penetrating peptides. For instance, neomycin could compete at PtdIns-4,5-P2 binding sites with proteins that bind and connect the plasma membrane to the actin cytoskeleton, resulting in the inhibition of endocytosis (42, 43). Therefore, at 37 °C, neomycin affected the peptide endocytosis pathway, the most efficient internalization pathway at these temperature and extracellular peptide concentrations (5 μM).

The neomycin effects observed at 4 °C were more difficult to explain because PtdIns-4,5-P2 is not only a key point in membrane trafficking and signaling. Indeed, neomycin as well as basic spermine, polylysine, and myristoylated alanine-rich C kinase substrate (amino acids 151–175) peptide, can sequester PtdIns-4,5-P2 and enhance the formation of acidic phospholipid lateral domains and lipid scrambling through PS exposure at the cell surface (41, 44). Therefore, all CPPs containing basic amino acids are also putative binders of PtdIns-4,5-P2 during the internalization process or once internalized.

Confocal Microscopy Imaging Does Not Reflect Concentrations of Internalized Peptides—Binding to negatively charged PtdIns-4,5-P2 or phosphatidylserine may be the reason why confocal microscopy imaging was not found reliable to assess CPP internalization efficiency. Indeed, we have shown herein and before (17) that despite experiments done in parallel and the use of the same tuning parameters for confocal microscopy, the relative fluorescence observed inside cells did not reflect the concentrations of intact internalized peptide. Indeed, it was shown here by mass spectrometry that neomycin decreased the kinetics of internalization at 37 °C of the Antp analogue P1, whereas a stronger fluorescent signal associated with the internalized CPP was observed by confocal microscopy imaging. Therefore, because the Antp analogue was not degraded within a 1-h incubation, the most plausible explanation for the difference observed between MALDI-TOF and confocal microscopy experiments is that neomycin binding to the negatively charged phospholipid PtdIns-4,5-P2 prevents the binding of the internalized cell-penetrating peptide to PtdIns-4,5-P2. This could lead to less fluorescence quenching (9) or better access to the biotin moiety linked to the CPP by streptavidin-Alexa Fluor 488 compared with the control experiment.

In summary, these data demonstrated that cell-penetrating peptides did translocate and internalize through endocytosis (Fig. 7) but to a different extent that depends on the peptide sequence (not the number of positive charges), extracellular peptide concentration, and membrane components. For Antp, translocation occurred at low extracellular peptide concentration, whereas endocytosis, a saturable and cooperative process, was activated at higher concentrations. There was no relationship between the high affinity of these peptides for cell membrane and their internalization efficacy. A direct involvement in the internalization process of the negatively charged PtdIns-4,5-P2 from the internal membrane leaflet, in relation with actin dynamics and endocytosis, has also been unveiled. Not only endocytosis but also translocation occurred in a narrow time window, which implied the specific recruitment of membrane components in both cases. For Antp, Tat, and R9, endocytosis principally involved GAG at the cell surface, whereas the membrane partners for translocation, likely lipids or glycosphingolipids, remain to be identified.

Acknowledgments—We thank Edmond Dupont and Alain Joliot for confocal microscopy imaging and the kind gift of neomycin.

REFERENCES

1. Derossi, D., Joliot, A. H., Chassaing, G., and Prochiantz, A. (1994) *J. Biol. Chem.* **269,** 10444–10450
2. Duchardt, F., Fotin-Mleczek, M., Schwarz, H., Fischer, R., and Brock, R. (2007) *Traffic* **8,** 848–866
3. Richard, J. P., Melikov, K., Vives, E., Ramos, C., Verbeure, B., Gait, M. J., Chernomordik, L. V., and Lebleu, B. (2003) *J. Biol. Chem.* **278,** 585–590
4. Vivès, E., Schmidt, J., and Pèlegrin, A. (2008) *Biochim Biophys Acta* **1786,** 126–138
5. Console, S., Marty, C., García-Echeverría, C., Schwendener, R., and Ballmer-Hofer, K. (2003) *J. Biol. Chem.* **278,** 35109–35114
6. Fuchs, S. M., and Raines, R. T. (2004) *Biochemistry* **43,** 2438–2444
7. Gump, J. M., and Dowdy, S. F. (2007) *Trends Mol. Med.* **13,** 443–448
8. Hällbrink, M., Oehlke, J., Papsdorf, G., and Bienert, M. (2004) *Biochim. Biophys. Acta* **1667,** 222–228
9. Ziegler, A., and Seelig, J. (2007) *Biochemistry* **46,** 8138–8145
10. Puckett, C. A., and Barton, J. K. (2009) *J. Am. Chem. Soc.* **131,** 8738–8739
11. Ivanov, A. I. (2008) *Methods Mol. Biol.* **440,** 15–33
12. Lee, H. L., Dubikovskaya, E. A., Hwang, H., Semyonov, A. N., Wang, H., Jones, L. R., Twieg, R. J., Moerner, W. E., and Wender, P. A. (2008) *J. Am. Chem. Soc.* **130,** 9364–9370
13. Burlina, F., Sagan, S., Bolbach, G., and Chassaing, G. (2006) *Nat. Protoc.* **1,** 200–205
14. Burlina, F., Sagan, S., Bolbach, G., and Chassaing, G. (2005) *Angew Chem. Int. Ed Engl.* **44,** 4244–4247
15. Delaroche, D., Aussedat, B., Aubry, S., Chassaing, G., Burlina, F., Clodic, G., Bolbach, G., Lavielle, S., and Sagan, S. (2007) *Anal. Chem.* **79,** 1932–1938
16. Dupont, E., Prochiantz, A., and Joliot, A. (2007) *J. Biol. Chem.* **282,** 8994–9000
17. Aubry, S., Burlina, F., Dupont, E., Delaroche, D., Joliot, A., Lavielle, S., Chassaing, G., and Sagan, S. (2009) *FASEB J.* **23,** 2956–2967
18. Aussedat, B., Sagan, S., Chassaing, G., Bolbach, G., and Burlina, F. (2006) *Biochim. Biophys. Acta* **1758,** 375–383
19. Théodore, L., Derossi, D., Chassaing, G., Llirbat, B., Kubes, M., Jordan, P., Chneiweiss, H., Godement, P., and Prochiantz, A. (1995) *J Neurosci.* **15,** 7158–7167
20. Saito, M., Iwamori, M., Lin, B., Oka, A., Fujiki, Y., Shimozawa, N., Kamoshita, S., Yanagisawa, M., and Sakakihara, Y. (1999) *Biochim. Biophys. Acta.* **1438,** 55–62
21. Rosales Fritz, V. M., Daniotti, J. L., and Maccioni, H. J. (1997) *Biochim. Biophys. Acta* **1354,** 153–158
22. Esko, J. D., Stewart, T. E., and Taylor, W. H. (1985) *Proc. Natl. Acad. Sci. U.S.A.* **82,** 3197–3201
23. Ter-Avetisyan, G., Tünnemann, G., Nowak, D., Nitschke, M., Herrmann, A., Drab, M., and Cardoso, M. C. (2009) *J. Biol. Chem.* **284,** 3370–3378
24. Poon, G. M., and Gariépy, J. (2007) *Biochem. Soc. Trans.* **35,** 788–793
25. Abes, R., Moulton, H. M., Clair, P., Yang, S. T., Abes, S., Melikov, K., Prevot, P., Youngblood, D. S., Iversen, P. L., Chernomordik, L. V., and Lebleu, B. (2008) *Nucleic Acids Res.* **36,** 6343–6354
26. Watkins, C. L., Schmaljohann, D., Futaki, S., and Jones, A. T. (2009) *Biochem. J.* **420,** 179–189
27. Ziegler, A., and Seelig, J. (2008) *Biophys. J.* **94,** 2142–2149
28. Yanagishita, M., and Hascall, V. C. (1992) *J. Biol. Chem.* **267,** 9451–9454
29. Iozzo, R. V. (1987) *J. Biol. Chem.* **262,** 1888–1900
30. Alves, I. D., Goasdoué, N., Correia, I., Aubry, S., Galanth, C., Sagan, S., Lavielle, S., and Chassaing, G. (2008) *Biochim. Biophys. Acta* **1780,** 948–959
31. Berlose, J. P., Convert, O., Derossi, D., Brunissen, A., and Chassaing, G. (1996) *Eur. J. Biochem.* **242,** 372–386
32. Wolkers, W. F., Looper, S. A., Fontanilla, R. A., Tsvetkova, N. M., Tablin, F., and Crowe, J. H. (2003) *Biochim. Biophys. Acta* **1612,** 154–163
33. Iglesias-Bartolomé, R., Crespo, P. M., Gomez, G. A., and Daniotti, J. L. (2006) *Febs J.* **273,** 1744–1758
34. Czech, M. P. (2000) *Cell* **100,** 603–606
35. Liu, A. P., and Fletcher, D. A. (2006) *Biophys. J.* **91,** 4064–4070
36. Haucke, V. (2005) *Biochem. Soc. Trans.* **33,** 1285–1289
37. Simonsen, A., Wurmser, A. E., Emr, S. D., and Stenmark, H. (2001) *Curr. Opin. Cell Biol.* **13,** 485–492
38. Nakase, I., Tadokoro, A., Kawabata, N., Takeuchi, T., Katoh, H., Hiramoto, K., Negishi, M., Nomizu, M., Sugiura, Y., and Futaki, S. (2007) *Biochemistry* **46,** 492–501
39. Gerbal-Chaloin, S., Gondeau, C., Aldrian-Herrada, G., Heitz, F., Gauthier-Rouvière, C., and Divita, G. (2007) *Biol. Cell* **99,** 223–238
40. Arbuzova, A., Martushova, K., Hangyás-Mihályné, G., Morris, A. J., Ozaki, S., Prestwich, G. D., and McLaughlin, S. (2000) *Biochim. Biophys. Acta* **1464,** 35–48
41. Goodyear, R. J., Gale, J. E., Ranatunga, K. M., Kros, C. J., and Richardson, G. P. (2008) *J Neurosci.* **28,** 9939–9952
42. Tkachenko, E., Lutgens, E., Stan, R. V., and Simons, M. (2004) *J. Cell Sci.* **117,** 3189–3199
43. Kirkpatrick, C. A., and Selleck, S. B. (2007) *J. Cell Sci.* **120,** 1829–1832
44. Bucki, R., Giraud, F., and Sulpice, J. C. (2000) *Biochemistry* **39,** 5838–5844